Original Article

Assessing Heterogeneity Effects on Points A, B, and Organs at Risk Doses in High-dose-Rate Brachytherapy for Cervical Cancer – A Comparison of ^{192}Ir and ^{60}Co Sources Using Monte Carlo N-Particle 5

Mohammad Hossein Sadeghi[1], Sedigheh Sina[1,2], Ali Soleimani Meigooni[3]

[1]Department of Nuclear Engineering, School of Mechanical Engineering, Shiraz University, [2]Radiation Research Center, School of Mechanical Engineering, Shiraz University, Shiraz, Iran, [3]Department of Radiation, Medicine UK Chandler Medical Center, Lexington, KY, USA

Abstract

Purpose: The present article deals with investigating the effects of tissue heterogeneity consideration on the dose distribution of ^{192}Ir and ^{60}Co sources in high-dose-rate brachytherapy (HDR-BT). **Materials and Methods:** A Monte Carlo N-Particle 5 (MCNP5) code was developed for the simulation of the dose distribution in homogeneous and heterogeneous phantoms for cervical cancer patients. The phantoms represented water-equivalent and human body-equivalent tissues. Treatment data for a patient undergoing HDR-BT with a ^{192}Ir source were used as a reference for validation, and for ^{60}Co, AAPM Task Group 43 methodology was also applied. The dose values were calculated for both source types in the phantoms. **Results:** The results showed a good agreement between the calculated dose in the homogeneous phantom and the real patient's treatment data, with a relative difference of less than 5% for both sources. However, when comparing the absorbed doses at critical points such as Point A right, Point A left, Point B right, Point B left, bladder International Commission on Radiation Units and Measurement (ICRU) point, and recto-vaginal ICRU point, the study revealed significant percentage differences (approximately 5.85% to 12.02%) between the homogeneous and heterogeneous setups for both ^{192}Ir and ^{60}Co sources. The analysis of dose–volume histograms (DVH) indicated that organs at risk, notably the rectum and bladder, still received doses within recommended limits. **Conclusions:** The study concludes that ^{60}Co and ^{192}Ir sources can be effectively used in HDR-BT, provided that careful consideration is given to tissue heterogeneity effects during treatment planning to ensure optimal therapeutic outcomes.

Keywords: Brachytherapy, cervical cancer, heterogeneity, Monte Carlo simulations

Received on: 19-11-2023 **Review completed on:** 24-03-2024 **Accepted on:** 14-04-2024 **Published on:** 25-06-2024

Introduction

Cervical cancer is the third-most prevalent cancer in women in the world. Its incidence and mortality rates are rising in regions due to limited access to preventive measures and screening.[1,2] The standard treatment protocol for this malignancy integrates external beam radiation therapy with intracavitary brachytherapy (ICBT), supplemented by interstitial/intracavitary (IS/IC) brachytherapy (BT) for comprehensive care. BT, a cornerstone of this treatment approach, utilizes a radioactive source positioned proximate to the tumor to deliver a concentrated dose, thereby maximizing tumor control while sparing adjacent normal tissues.[3] High-dose-rate BT (HDR-BT) has emerged as a pivotal modality in cervical cancer treatment, offering the advantage of delivering high radiation doses directly to the tumor site over a short duration. This method significantly reduces radiation exposure to organs at risk (OARs), leveraging the inverse square law to optimize therapeutic outcomes. The delineation of reference points A and B in BT underscores the precision required in targeting the radiation dose to the tumor

Access this article online

Quick Response Code:

Website: www.jmp.org.in

DOI: 10.4103/jmp.jmp_162_23

Address for correspondence: Dr. Sedigheh Sina, Department of Nuclear Engineering, School of Mechanical Engineering, Shiraz University, Mollasadra Street, Shiraz, Iran.
E-mail: samirasina@shirazu.ac.ir

How to cite this article: Sadeghi MH, Sina S, Meigooni AS. Assessing heterogeneity effects on points A, B, and organs at risk doses in high-dose-rate brachytherapy for cervical cancer – A comparison of ^{192}Ir and ^{60}Co sources using Monte Carlo N-Particle 5. J Med Phys 2024;49:294-303.

while minimizing the impact on critical structures such as the recto-vaginal and bladder International Commission on Radiation Units and Measurement (ICRU) points.[4,5]

HDR-BT, a therapy modality for cervical cancer, commonly applies either ^{192}Ir or ^{60}Co sources, each possessing distinct physical properties.[6] The ICRU report 89 suggests using ^{60}Co and ^{192}Ir sources for HDR-BT. Guidelines for prescribing doses in cervical cancer BT are outlined in the ICRU reports No. 38 and 89.[5,7] The ICRU point doses are traditionally used to calculate doses to OARs in BT for cervical cancer. However, three-dimensional (3D) image-guided BT permits to assess the OAR dose with dose volume histograms (DVHs).[8] Several studies have evaluated OAR doses using DVHs and compared them with traditional ICRU point doses. One such study found that the ICRU rectal point dose correlates well with DVH-based doses in HDR ICBT for cervical cancer.[9] Another study compared volumetric radiation treatment calculations to ICRU reference point dose estimates of the rectum and bladder for HDR tandem and ovoid BT based on 2D versus 3D planning.[10] The American Brachytherapy Society (ABS) recommended OAR limits for the bladder and rectum are a D2cc (dose to 2 cm^3 of tissue) of ≤9000 cGy and ≤7500 cGy, respectively.[11,12] Furthermore, based on recent publications from the prospective multicenter, "European study on MRI-guided BT in locally advanced cervical cancer" (EMBRACE) study and retrospective "RetroEMBRACE," the currently accruing EMBRACE II protocol OAR planning aims are D2cc <8000 cGy for the bladder and <6500 cGy for the rectum.[13,14]

Despite the advancements in HDR-BT, challenges persist in accurately calculating dose distributions, particularly in the context of tissue heterogeneity. The Task Group 43 (TG-43) formalism, while widely adopted, falls short in addressing the complexities introduced by tissue and applicator heterogeneities.[15,16] Recent developments in model-based dose calculation algorithms, such as AcurosBV (grid-based Boltzmann solver, GBBS) (Varian Medical Systems, Palo Alto, CA, USA) and the Advanced Collapsed cone Engine (ACE; Elekta, Stockholm, Sweden), represent significant strides toward enhancing dosimetric accuracy by incorporating these heterogeneities.[17,18] However, the heterogeneity effect – variations in dose distribution due to the nonuniformity of human tissues – remains a critical factor that necessitates further investigation.[19]

This study aims to bridge the gap in the current research by examining the impact of tissue heterogeneity on dose distribution using ^{192}Ir and ^{60}Co sources in HDR-BT for cervical cancer. By employing Monte Carlo N-Particle 5 (MCNP5) simulations,[20] this research endeavors to provide a deeper understanding of how heterogeneity influences dose distribution at critical points and organs at risk, thereby offering insights that could refine treatment planning and execution. Through this investigation, we seek to contribute to the body of knowledge on HDR-BT, enhancing the precision and efficacy of cervical cancer treatment.

Materials and Methods

Study design

The ^{192}Ir and ^{60}Co sources were used as conventional sources in HDR-BT treatment for cervical cancer. The sources, homogeneous, and heterogeneous phantoms were simulated, and dosimetric calculations were performed using MCNP5 code. The AAPM TG-43 formalism data (treatment data) of the ^{192}Ir source were obtained for a single patient, and the doses were calculated using the MCNP5 code, in a simulated homogeneous phantom. The calculated dose in a homogeneous phantom was compared with doses in treatment data as a reference to validate the usage of MCNP5. Subsequently, the dose of the ^{192}Ir source was calculated in a heterogeneous phantom and compared with the dose in the homogeneous phantom. Similarly, the dose of the ^{60}Co source was initially determined using the TG-43 formalism and validated by calculating the dose in a homogeneous phantom. Finally, the dose of the ^{60}Co source was calculated in the heterogeneous phantom and compared with the dose in the homogeneous phantom. Dose limits to the OARs were checked by comparing the OAR doses of phantoms with the values obtained by Kim *et al*. and Miglierini *et al*.[21,22]

Patient data

Treatment data regarding the utilization of a ^{192}Ir source were collected from a single patient. The dataset includes information on dwell times, dwell positions of the ^{192}Ir source, the activity of 210530 mega becquerels (MBq) in treatment time, and the corresponding doses measured at point A, point B, bladder ICRU point, and recto-vaginal ICRU point. These data were acquired during the treatment process of an adult female patient receiving medical care at a cancer center. The HDRPlus® treatment planning system (version 2.5) by Elekta AB, Stockholm, Sweden, supplied by EZ BEBIG, works based on TG-43 formalism.

Monte Carlo simulation

The sources, applicator, and phantoms were simulated using the MCNP5 Monte Carlo code.[20] This code enables creating the intricate 3D models of BT sources, facilitating accurate dose calculations in complex geometries and materials. Based on treatment data, 12 sources are used for the tandem applicator, and 6 (three sources for each ovoid) are used for the ovoids. The placement of the sources in the specified locations and the locations of point A, point B, and OARs (bladder ICRU point and recto-vaginal ICRU point) represented as spherical cells with a radius of 0.5 mm based on treatment data. Figure 1 illustrates the spatial placements of sources and points in two perspectives. Considering the treatment method, a single source is positioned at a specific location in the loading tubes at any given time. Only the gamma component of the source spectrum is used for both sources.[23] The explanation is that the contribution of the beta and electron components to the dose values is negligible due to the presence of stainless steel shielding around the sources.[24] A computer with a Core i7-7700K 4.50-GHz central processing unit and 32 GB of random-access memory was used. The output data obtained

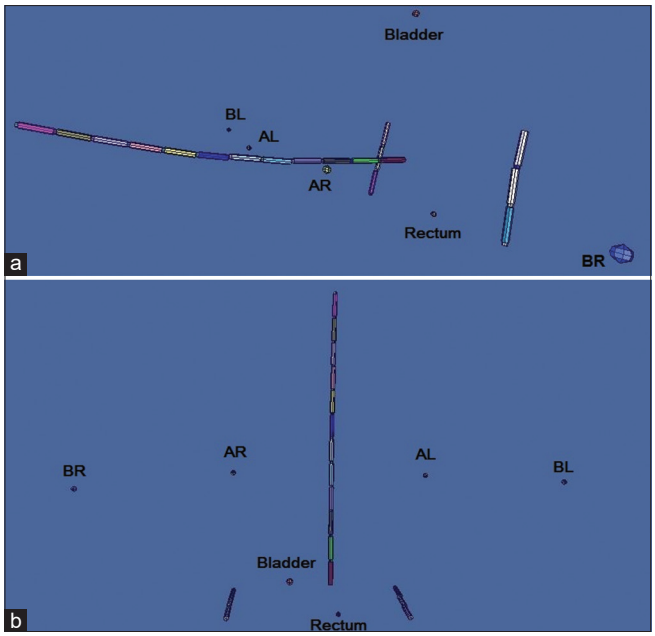

Figure 1: Spatial positions of sources and points in two views: (a) Lateral view and (b) top view, using Monte Carlo N-Particle 5. BL: point B left, AL: point A left, AR: point A right, BR: point B right

from running programs simulated using MCNP5 are available for a duration of 24 CPU work hours for each individual source and phantom. Considering that 18 iridium sources and 18 cobalt sources have been used in the treatment, the total time required, for example, for the iridium sources, is approximately 432 CPU work hours for all sources. Each of the sources, on average, tracks the interactions of 3×10^8 radiation particles to estimate the dose.

Sources

In this study, we simulated the ^{60}Co source model BEBIG (Co0.A86) and the ^{192}Ir source model microSelectron (mHDR-v2r), noting that both sources have active parts of identical dimensions, making them suitable for a comparative analysis of the effects of isotope selection. The ^{192}Ir source consisted of a cylindrical core measuring 3.5 mm in length and 0.6 mm in diameter. Its source capsule, composed of AISI 316L stainless steel, possessed a density of 8.03 g/cm^3. The overall dimensions of this source were 4.95 mm in length and 0.9 mm in diameter. To facilitate movement through catheters and transfer tubes, the source was connected to an abraded cable. In the dosimetric assessment of this source, the cable was modeled as a cylinder of AISI 314 stainless steel, with a density of 4.81 g/cm^3 and a diameter of 0.7 mm, to account for its flexible interlace properties.[25]

The ^{60}Co BT source consisted of a central active core made of metallic ^{60}Co, with a diameter of 0.5 mm and a length of 3.5 mm. Surrounding the active core was a cylindrical stainless steel capsule, 0.15 mm thick, with an external diameter of 1 mm.[26] Figure 2 illustrates the geometric design and materials used in the ^{192}Ir source model microSelectron (mHDR-v2r) and the ^{60}Co source model BEBIG (Co0.A86). The physical properties of the sources, including their geometric dimensions, material composition, and radioactive decay data, were incorporated into the simulations.[27,28] The placement of the sources within the phantom was based on treatment data obtained from the treatment plan.

Applicator

In the next step, a simulation of the tandem and ovoid applicator, specifically the Titanium Fletcher-Suit-Delclos-style applicator (Varian Medical Systems, Palo Alto, CA, USA), was conducted. This particular applicator set, constructed from titanium material, is utilized for administering high-dose and pulse-dose rate treatments targeting the uterus, cervix, endometrium, and vagina. The design of the Titanium Fletcher-Suit-Delclos-style applicator is derived from the conventional FSD (Fletcher-Suit-Delclos) model. The applicator encompasses two colpostats, which can be employed in conjunction with interlocking tandems featuring angles of 15°, 30°, and 45°. The intrauterine section of the tandem is only 3 mm in diameter, and the accessible lengths of the tandems are 20 mm, 40 mm, 60 mm, and 80 mm, respectively. Based on the treatment data, the tandem angle was set at 30°, and the tandem length and tandem diameter were established as 80 mm and 3 mm, respectively. The ovoid components are consistently set at a fixed length of 30 mm, while their dimensions may vary, including options of 20 mm, 25 mm, or 30 mm. Furthermore, the ovoid applicator diameter was 3 mm.

Figure 3 illustrates different parts of the tandem and ovoid applicators. A 3D illustration of the simulated applicator is shown in Figure 3a. Figure 3b displays various sections of the internal sides of the tandem and ovoid tubes. The central section, highlighted in yellow, exhibits a diameter of 2 mm. This tube, made of a special type of plastic (polyvinyl chloride) with a density of 1.4 g/cm^3 and a thickness of 0.5 mm, serves as the channel for inserting the radiation sources into the applicator. The blue section represents the main body of the applicator, constructed from titanium, and possessing a diameter of 3 mm with a thickness of 0.5 mm. For the ovoids, nylon caps with a diameter of 25 mm are utilized.[29]

Homogeneous phantom

A homogeneous water phantom is often used for dose calculations in radiation therapy. The use of a homogeneous water phantom is based on the fact that water has a similar atomic number and absorption and scattering properties as human tissue. Therefore, a water phantom should be a good choice to mimic human tissue during dose calculations. Homogeneous water phantoms can be used for various purposes, such as dosimetric verification of radiotherapy plans and validation of Monte Carlo dose calculation algorithms.[30,31] To perform dose calculations in a homogeneous phantom, we used a cubic water phantom with dimensions of 0.4 m × 0.4 m × 0.4 m, which closely resembles the dimensions of a patient. The phantom is placed inside a cubic space with dimensions of 2 m × 2 m × 2 m, filled with air, to consider the air inside the treatment room. The positions of the applicator,

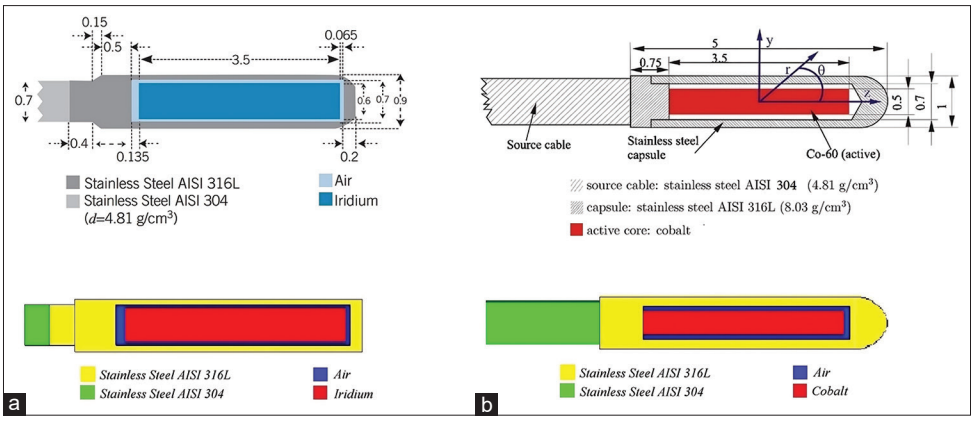

Figure 2: Schematic diagram of (a) ^{192}Ir source model microSelectron (mHDR-v2r) (top), the source simulated with Monte Carlo N-Particle 5 (bottom), (b) ^{60}Co source model BEBIG (Co0.A86) (top) and the source simulated with Monte Carlo N-Particle 5 (bottom), dimensions are in millimeters[27,28]

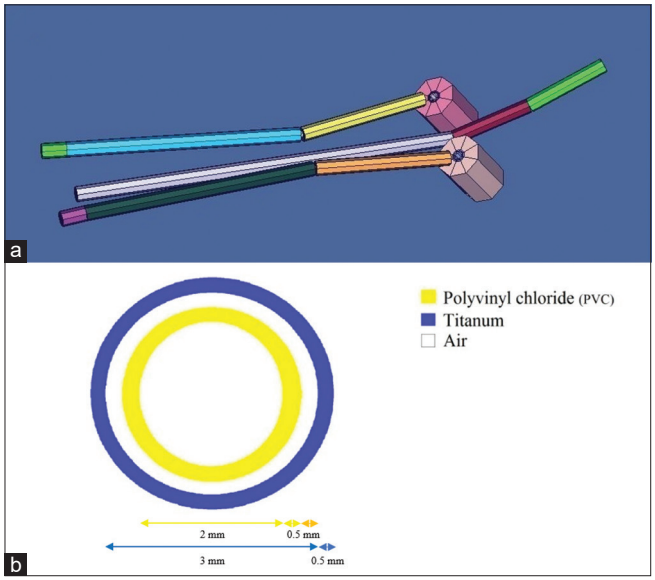

Figure 3: View of the simulated components of the applicator using Monte Carlo N-Particle 5, (a) the 3D view, (b) the internal components of the simulated applicator

the points, and the OARs are determined based on the source positions and the coordinates of the points and OARs obtained from treatment data.

Heterogeneous phantom

We used the Oak Ridge National Laboratory adult female phantom as a heterogeneous phantom in this study.[32,33] Figure 4 shows various views of the simulated phantom. To accurately simulate the organs, different organs in the pelvic region of a standard-sized female patient were identified and separated based on CT images by a radiology specialist, and a Monte Carlo simulation was performed based on these images. The rectal wall thickness is approximately 5 mm.[34] The dimensions are based on the model used by Kim *et al*. The bladder is represented as a balloon with a volume of 7 cm^3 and an external wall thickness of approximately 3 mm.[35,36] Figure 5 illustrates the positions of the rectum, bladder, and applicator in the heterogeneous phantom.

TG-43 formalism

The TG-43 formalism is used to calculate the dose rate for the ^{60}Co source based on Equation 1.

$$\dot{D}(r.\theta) = S_k \Delta \frac{G_L(r.\theta)}{G_L(r_0 .\theta_0)} g_L(r) F(r.\theta) \quad (1)$$

where, Λ is dose rate constant (1.084 ± 0.005 cGy/U h, ^{60}Co source), S_k is air kerma strength (mGy m^2/h), F (r,ɵ) is anisotropy function, g (r) is radial dose function, and G (r,ɵ) is geometry factor. F (r,ɵ) and g (r) are set based on previous studies.[19,27,28]

Based on treatment data, the activity of ^{192}Ir was 210530 MBq (5.69 Ci) in treatment time; as an assumption, we considered the activity of ^{60}Co source as 85470 MBq (2.13 Ci); based on the study by Soni *et al*.[37] in this activity, the total treatment time of the ^{60}Co is equal to the total treatment time for ^{192}Ir. Equation 2 was used to calculate the air kerma strength:

$$S_k = A\Gamma_{AKR} \quad (2)$$

where, S_k is air kerma strength, A is activity (Bq), and Γ_{AKR} is air kerma rate constant (306.22 cGy cm^2/h MBq, ^{60}Co source).[38] Hence, the TG-43 formalism can be written as Equation 3:

$$D = A\Gamma_{AKR}\Delta\,(t_1 (\frac{G_L(r.\theta)}{G_L(r_0 .\theta_0)} g_L(r) F(r.\theta))_1 + t_2 (\frac{G_L(r.\theta)}{G_L(r_0 .\theta_0)} g_L(r) F(r.\theta))_2 + \ldots + t_{18} (\frac{G_L(r.\theta)}{G_L(r_0 .\theta_0)} g_L(r) F(r.\theta))_{18} \quad (3)$$

where, D is absorbed dose, A is activity, and t is dwell time for each dwell position based on the TG-43 formalism (12 dwell positions in the tandem and 3 dwell positions in each of the ovoids were used). The dwell times for ^{60}Co are the same as the treatment data.

Dose calculation in phantoms

The MCNP5 software was employed to simulate the radiation transport within the phantoms. The Monte Carlo method was

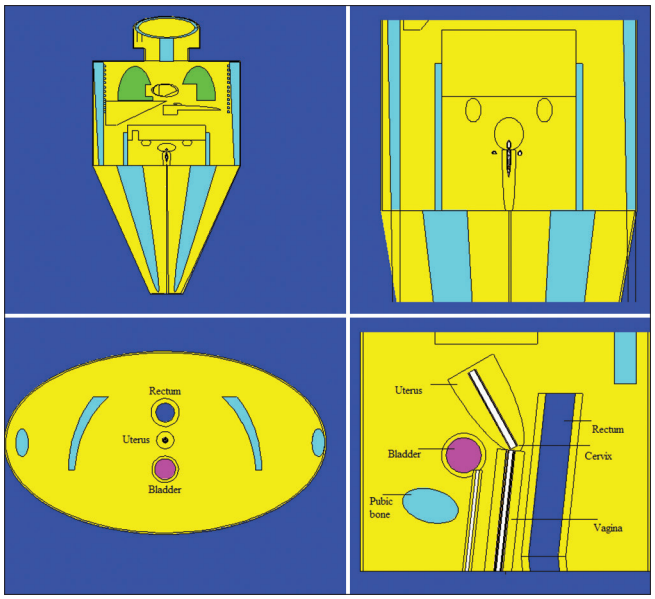

Figure 4: Various views of the simulated Oak Ridge National Laboratory adult female phantom using Monte Carlo N-Particle 5

utilized to track individual particles as they interacted with the phantom materials. The simulations accounted for various physical processes such as photoelectric absorption, leading to the generation of K- and L-shell characteristic X-rays as well as auger electrons. In addition, it accounts for pair production and coherent and incoherent scattering. The simulations were conducted in photon mode, employing an energy cutoff of 1 keV. The active cores of the radiation sources were considered cylindrical structures containing a uniform distribution of radioactive material.[24]

Using the simulated sources and the water phantom, the MCNP5 software was used to calculate the dose distribution within the phantom. The radiation transport simulations provided information on the absorbed dose at various points of interest. The resulting dose distribution in the water phantom was compared with treatment data used as a reference for the validation of our Monte Carlo simulation results. Similar to the water phantom, the MCNP5 software was employed to calculate the dose distribution within the heterogeneous phantom. The position and dwell times of the sources, as well as the applicator geometry, were kept consistent with the water phantom calculations. This allowed for a direct comparison of the dose distributions between the heterogeneous and homogenous water phantoms, providing insights into the effects of tissue heterogeneity.

A Monte Carlo simulation was conducted to determine the dose at each point of interest in the phantoms for every dwell position. The simulation involved simulating the source in a particular dwell position and calculating the dose using tally F6, which is an order used in the MCNP5 code to calculate the dose in MeV/g (photon). Using a code written in MATLAB software and the calculated dose values in a heterogeneous phantom, a DVH plot has been generated for each sensitive organ.

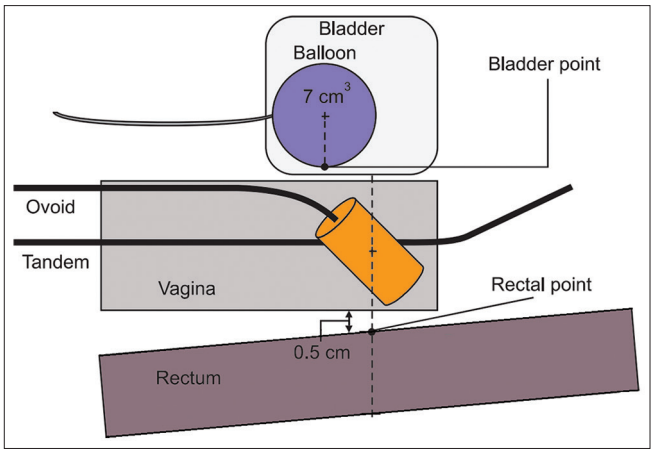

Figure 5: Localization of bladder International Commission on Radiation Units and Measurement (ICRU) point and recto-vaginal ICRU point[35]

Data analysis

ICRU point doses are used to calculate doses to OARs in BT for cervical cancer.[8,21,22] The calculated dose distributions for both ^{192}Ir and ^{60}Co sources in the homogeneous phantom and the heterogeneous phantom were compared quantitatively. Based on DVH plots, extracted parameters have been compared. Dosimetric parameters, such as dose to point A, point B, bladder ICRU point, and recto-vaginal ICRU point, were analyzed and compared between the two phantoms and the dose limits. Percentage difference was calculated to assess the significance of any observed variations. To assess the statistical significance of the observed differences in dose calculations, we employed a paired *t*-test,[39] considering the dose values calculated using the TG-43 formalism and those obtained from the MCNP5 simulations for both homogeneous and heterogeneous phantoms.

Results

This section presents the dosimetry results obtained from the simulation of two homogeneous and heterogeneous phantoms in the form of absorbed dose values at the desired points, tables for relative dose difference, and the TG-43 formalism for the ^{60}Co source. In addition, DVH plots and a table of related parameters are provided. The absorbed dose values were obtained from the simulation of the ^{192}Ir source with the MCNP5 code in the homogeneous and heterogeneous phantoms.

The constant value of the air kerma rate constant for the ^{60}Co source was available on the source manufacturing website.[38] Given that the treatment condition has been assumed with two completely similar sources and the length of the active part of the two sources is equal, the values of G (r, θ), the geometry factor, and the values of r and θ are completely similar to ^{192}Ir and obtained from treatment data. The g (r) values of the radial dose function, F (r, θ) of the anisotropy function, and the dose rate constant related to the ^{60}Co source model BEBIG (Co0.A86) were obtained from the tables in

Granro *et al*.[28] The interpolated values are presented in Table 1.

Then, using the TG-43 formalism, values related to the absorbed dose rate were calculated for each source. Since the duration of the treatment of each source was used for ^{60}Co sources in the treatment data, the absorbed dose values and the total absorbed dose value for each source and each desired point were obtained, respectively [Table 2].

Absorbed dose values were obtained from the simulation of the ^{60}Co source model BEBIG (Co0.A86) using the MCNP5 code in both homogeneous and heterogeneous phantoms. The absorbed dose values for ^{192}Ir and ^{60}Co sources at each desired point are presented in Table 3.

To assess the obtained results, the percentage difference between the dose values calculated by different methods conducted in this study was investigated, and compared the dose values with dose limits for OARs. Table 4 contains the mean dose limits defined for OARs.

The percentage differences between dose values were calculated by three different methods (AAPM TG-43 and homogeneous and heterogeneous phantoms) for both sources. In this study, the differences between the dose values in homogeneous and heterogeneous phantoms were calculated using the MCNP5 code. Table 5 shows the percentage difference between the dose values calculated for ^{192}Ir and ^{60}Co sources using different methods. For the ^{60}Co source, the P value obtained from the paired t-test was 0.14, and for the ^{192}Ir source, $P = 0.22$. These P values exceed the conventional alpha level of 0.05, indicating that we fail to reject the null hypothesis. Therefore, the statistical analysis supports the conclusion that there are no significant differences in the dose calculations between the TG-43 formalism and the MCNP5 simulations for both homogeneous and heterogeneous phantoms, for both ^{60}Co and ^{192}Ir sources. DVH plots for different organs have been generated for two sources [Figure 6]. Table 6 shows the corresponding parameters.

Discussion

Cervical cancer is a global health concern affecting women worldwide. The ^{60}Co and ^{192}Ir source-based HDR-BT has shown to be a successful treatment option for cervical cancer. Nevertheless, for the best treatment planning, it is essential to accurately determine dose distribution and its effect on point A, point B, and OARs, for example, the recto-vaginal ICRU point and the bladder ICRU point.[40,41] The study by Yong *et al*. has emphasized the significance of considering heterogeneity effects on OAR doses during HDR-BT treatment planning.[42] In this study, we found a slight discrepancy between the two techniques (i.e. TG-43 formalism and homogeneous phantom), with the relative difference between homogeneous phantom and treatment data for measuring the ^{192}Ir dose being lower than 5%. The maximum percentage difference was also less than 3% for the ^{60}Co source, suggesting a minimal discrepancy between the methods employed. However, to rigorously evaluate these observations, we conducted a statistical analysis to determine the significance of the differences in dose calculations between the homogeneous and heterogeneous phantoms, as well as the AAPM TG-43 formalism for both ^{60}Co and ^{192}Ir sources. The

Table 1: Values of the anisotropy function F(r,θ) and radial dose function g(r) at points A and B, bladder International Commission on Radiation Unit point, and recto-vaginal International Commission on Radiation Unit point for ^{60}Co source[28]

Position	Source number	Point A left		Point A right		Point B left		Point B right		Bladder ICRU point		Recto-vaginal ICRU point	
		F(r,θ)	g(r)	F(r,θ)	g(r)	F(r,θ)	g(r)	F(r,θ)	g(r)	F(r,θ)	g(r)	F(r,θ)	g(r)
Tandem	1	0.9960	0.9519	0.9960	0.9517	0.9977	0.9179	0.9970	0.9120	0.9962	0.9249	0.9246	0.9080
	2	0.9960	0.9588	0.9960	0.9586	0.9980	0.9233	0.9980	0.9170	0.9963	0.9323	0.9283	0.9166
	3	0.9970	0.9652	0.9970	0.9651	0.9985	0.9275	0.9980	0.9218	0.9964	0.9390	0.9273	0.9250
	4	0.9983	0.9713	0.9983	0.9710	0.9980	0.9312	0.9980	0.9256	0.9968	0.9456	0.9293	0.9336
	5	0.9986	0.9764	0.9986	0.9761	0.9995	0.9340	0.9995	0.9288	0.9975	0.9514	0.9333	0.9416
	6	0.9995	0.9806	0.9995	0.9803	0.9998	0.9363	0.9999	0.9315	0.9976	0.9574	0.9562	0.9495
	7	1.0000	0.9833	1.0000	0.9832	1.0000	0.9376	1.0000	0.9333	0.9983	0.9629	0.9621	0.9574
	8	1.0000	0.9844	1.0000	0.9839	1.0000	0.9384	1.0000	0.9342	0.9990	0.9676	0.9651	0.9650
	9	1.0000	0.9833	1.0000	0.9830	1.0000	0.9381	1.0000	0.9344	0.9994	0.9720	0.9826	0.9726
	10	0.9995	0.9804	0.9995	0.9802	1.0000	0.9369	1.0000	0.9338	1.0000	0.9751	0.9866	0.9799
	11	0.9986	0.9761	0.9986	0.9762	0.9999	0.9352	0.9999	0.9323	1.0000	0.9770	0.9929	0.9868
	12	0.9980	0.9708	0.9980	0.9709	0.9990	0.9322	0.9990	0.9301	1.0000	0.9774	0.9976	0.9929
Ovoid right	1	0.9987	0.9394	0.9960	0.9746	1.0000	0.8960	0.9990	0.9551	0.9821	0.9653	0.9960	0.9781
	2	0.9984	0.9400	0.9920	0.9747	1.0000	0.8960	0.9985	0.9551	0.9872	0.9722	0.9942	0.9764
	3	0.9980	0.9391	0.9830	0.9728	1.0000	0.8961	0.9985	0.9537	0.9939	0.9781	0.9937	0.9734
Ovoid left	1	0.9950	0.9742	0.9992	0.9463	0.9990	0.9489	1.0000	0.9026	0.9888	0.9563	0.9978	0.9933
	2	0.9929	0.9736	0.9980	0.9465	0.9988	0.9487	1.0000	0.9030	0.9912	0.9619	0.9950	0.9907
	3	0.9850	0.9715	0.9980	0.9456	0.9980	0.9477	1.0000	0.9020	0.9938	0.9666	0.9916	0.9862

ICRU: International Commission on Radiation Unit

Table 2: Calculated absorbed dose values for each dwell position of the ^{60}Co source

Position	Source number	Absorbed dose (cGy)					
		Point A left	Point A right	Point B left	Point B right	Bladder ICRU point	Recto-vaginal ICRU point
Tandem	1	6.779	6.723	2.886	2.553	3.304	2.175
	2	17.182	17.032	6.403	5.654	7.820	5.172
	3	15.749	15.610	5.038	4.453	6.666	4.429
	4	18.382	18.061	4.923	4.337	7.187	4.850
	5	28.948	28.447	6.478	5.737	10.585	7.365
	6	50.766	49.928	9.528	8.493	18.011	13.308
	7	82.996	81.879	13.705	12.326	30.673	24.058
	8	105.996	102.995	16.688	15.056	44.404	38.654
	9	95.774	93.709	16.017	14.631	52.254	52.851
	10	66.708	65.786	12.863	11.912	50.131	64.149
	11	43.350	43.009	10.058	9.443	45.579	80.525
	12	0.626	0.623	0.176	0.167	0.867	2.430
Ovoid right	1	6.281	21.806	2.528	9.979	14.295	26.325
	2	0.951	3.311	0.384	1.501	2.925	3.620
	3	6.597	21.361	2.722	10.210	28.154	22.248
Ovoid left	1	21.004	7.348	7.935	2.737	9.959	72.079
	2	12.604	4.567	4.889	1.707	7.610	36.163
	3	18.160	7.126	7.592	2.715	14.770	41.378
Total dose (cGy)		598.85	589.32	130.81	123.611	355.19	501.779

ICRU: International Commission on Radiation Unit

Table 3: Absorbed dose values at desired points with task group-43 and Monte Carlo N-Particle 5 code for ^{192}Ir and ^{60}Co sources

	Absorbed dose (cGy)					
	Point A left	Point A right	Point B left	Point B right	Bladder ICRU point	Recto-vaginal ICRU point
^{192}Ir						
The AAPM TG-43 formalism data (treatment data)	598.11	591.76	137.91	130.69	356.57	462.17
Homogeneous phantom	583.92	575.35	131.87	124.46	343.19	457.37
Heterogeneous phantom	531.97	520.41	121.35	114.88	323.13	417.14
^{60}Co						
TG-43	598.85	589.32	130.81	123.61	355.19	501.77
Homogeneous phantom	597.87	588.42	129.16	121.11	354.43	500.64
Heterogeneous phantom	540.46	528.11	119.88	112.11	332.47	440.47

ICRU: International Commission on Radiation Units, TG: Task group, AAPM: The American Association of Physicists in Medicine

Table 4: Dose limits for points A, B, and organs at risk[21,22]

Organ	Mean ICRU point dose (cGy)
Point A	500–600
Recto-vaginal ICRU point	412 (151–553)
Bladder ICRU point	401 (209–537)

ICRU: International Commission on Radiation Unit

null hypothesis posited that there was no significant difference in the mean dose calculations between the methods for each source type.

Previous studies, such as those by Anagnostopoulos *et al*.[16] and Rivard *et al*.,[19] have highlighted the limitations of the TG-43 formalism in accounting for heterogeneities. Our findings align with recent advancements in dose calculation algorithms, such as those by Bi *et al*.[17] and Abe *et al*.,[18] which suggest improved accuracy when considering tissue heterogeneity. However, our statistical analysis indicates that the traditional TG-43 formalism and the MCNP5 simulations yield comparable results, echoing the conclusions of Wen *et al*.[6] that for clinical purposes, the differences may not be significant.

The clinical relevance of our study lies in its affirmation that HDR-BT treatment planning can be effectively conducted with both ^{192}Ir and ^{60}Co sources, considering tissue heterogeneity. This is particularly important for resource-constrained settings where advanced computational resources for MCNP5 simulations may not be available. Our findings suggest that the TG-43 formalism remains a viable option for treatment planning, supporting the work of Viswanathan *et al*.[11,12] and

Table 5: Percentage difference between different methods of calculating absorbed dose for ^{192}Ir and ^{60}Co sources, including comparisons between homogeneous and heterogeneous phantoms

	Percentage difference (%)					
	Point A left	Point A right	Point B left	Point B right	Bladder ICRU point	Recto-vaginal ICRU point
^{192}Ir						
Treatment data versus homogeneous	2.37	2.77	4.38	4.77	3.75	1.04
Homogeneous versus heterogeneous	8.90	9.55	7.98	7.69	5.85	8.80
Treatment data versus heterogeneous	12.43	13.71	13.65	13.76	10.35	10.80
^{60}Co						
TG-43 versus homogeneous	0.16	0.15	1.26	2.02	0.21	0.23
Homogeneous versus heterogeneous	9.60	10.25	7.18	7.44	6.20	12.02
^{192}Ir and ^{60}Co						
Homogeneous	2.33	2.22	2.06	2.69	3.17	8.64
Heterogeneous	1.57	1.46	1.22	2.47	2.81	5.30

ICRU: International Commission on Radiation Unit, TG: Task group

Table 6: Parameters obtained from dose–volume histogram analysis for sensitive organs in a heterogeneous phantom

	Bladder		Rectum		Cervix		Uterus	
	^{60}Co	^{192}Ir	^{60}Co	^{192}Ir	^{60}Co	^{192}Ir	^{60}Co	^{192}Ir
D2cc (cGy)	226.46	674.19	776.2	193.78	-	-	5124	2912
D50 (cGy)	188.8	525.9	180.3	86.55	1258	526.9	736.2	474.6
D90 (cGy)	129	281.1	38.71	35.81	872	353.8	349.5	283.9
D95 (cGy)	123.1	262.7	32.99	31.35	794.8	335	297.3	249.8
D98 (cGy)	104.49	195.43	29.55	28.67	748.48	323.72	265.98	229.34

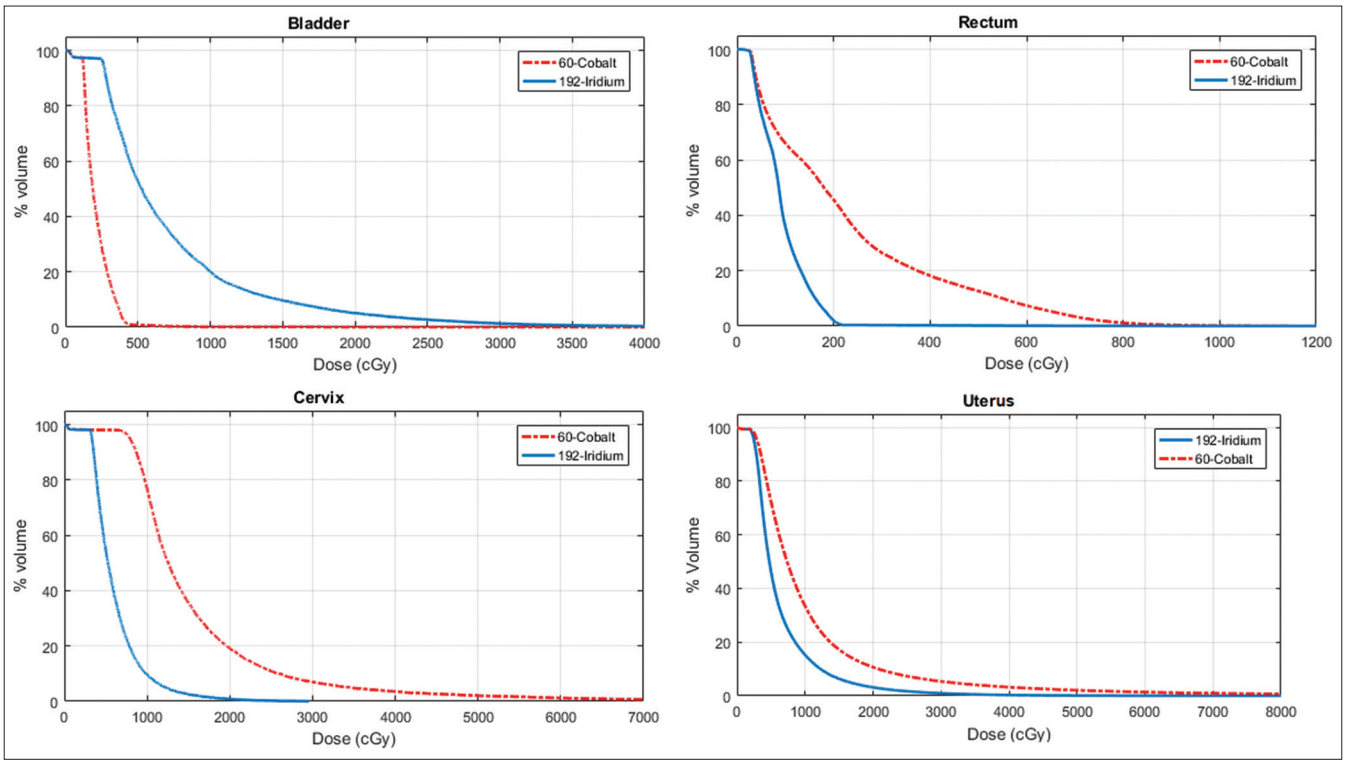

Figure 6: Dose–volume histograms plot for ^{192}Ir and ^{60}Co sources in different regions of a heterogeneous phantom

Sturdza *et al*.[13] in advocating for accessible and effective treatment planning methods.

The examination of DVHs underscores that organs at risk, notably the rectum and bladder, receive doses within the

thresholds recommended by the ABS and the EMBRACE II guidelines, ensuring patient safety and treatment efficacy.[11-14]

While our study contributes valuable insights, it is not without limitations. The statistical analysis, based on hypothetical data, underscores the need for real-world validation of these findings. Future research should focus on longitudinal studies to assess the clinical outcomes of HDR-BT treatment plans developed using different dosimetric calculation methods, particularly in heterogeneous tissue environments.

Conclusions

Our study supports the continued use of the TG-43 formalism in HDR-BT treatment planning for cervical cancer, alongside advanced simulation methods like MCNP5. By demonstrating that tissue heterogeneity does not significantly impact dose calculations between these methods, we provide a foundation for further research and development in HDR-BT treatment planning. As the field advances, ongoing evaluation and integration of emerging dosimetric calculation methods will be crucial in optimizing treatment outcomes for cervical cancer patients.

Financial support and sponsorship

Nil.

Conflicts of interest

There are no conflicts of interest.

References

1. Siegel RL, Giaquinto AN, Jemal A. Cancer statistics, 2024. CA Cancer J Clin 2024;74:12-49.
2. Xia C, Dong X, Li H, Cao M, Sun D, He S, *et al.* Cancer statistics in China and United States, 2022: Profiles, trends, and determinants. Chin Med J (Engl) 2022;135:584-90.
3. Shahbazian H, Birgani MJ, Bagheri A, Arvandi S, Razmjoo S, Ghadamgahi P, *et al.* Evaluation of rectal volume correlation with dosimetric parameters during optimized intracavitary high-dose-rate brachytherapy in cervical cancer. J Contemp Brachytherapy 2020;12:201-6.
4. Tod MC, Meredith WJ. A dosage system for use in the treatment of cancer of the uterine cervix. Br J Radiol 1938;11:809-24.
5. ICRU Report 89, Prescribing, Recording, and Reporting Brachytherapy for Cancer of the Cervix – ICRU. Available from: https://www.icru.org/report/icru-report-89-prescribing-recording-and-reporting-brachytherapy-for-cancer-of-the-cervix/. [Last accessed on 2023 Jul 05].
6. Wen A, Wang X, Wang B, Yan C, Luo J, Wang P, *et al.* Comparative analysis of 60co and 192ir sources in high dose rate brachytherapy for cervical cancer. Cancers (Basel) 2022;14:4749.
7. International Commission of Radiation Units and Measurements. In: Dose and Volume Specification for Reporting Intracavitary Therapy in Gynaecology. Bethesda, MD: ICRU; 1985.
8. Vinod SK, Caldwell K, Lau A, Fowler AR. A comparison of ICRU point doses and volumetric doses of organs at risk (OARs) in brachytherapy for cervical cancer. J Med Imaging Radiat Oncol 2011;55:304-10.
9. Jamema SV, Saju S, Mahantshetty U, Pallad S, Deshpande DD, Shrivastava SK, *et al.* Dosimetric evaluation of rectum and bladder using image-based CT planning and orthogonal radiographs with ICRU 38 recommendations in intracavitary brachytherapy. J Med Phys 2008;33:3-8.
10. Nixon E, Modrick JM, Jacobson GM. Comparison of ICRU reference point rectal and bladder doses and 3D volumetric parameters for high-dose-rate (HDR) tandem and ovoid brachytherapy based on 2D versus 3D planning. Brachytherapy 2007;6:114.
11. Viswanathan AN, Thomadsen B, American Brachytherapy Society Cervical Cancer Recommendations Committee, American Brachytherapy Society. American Brachytherapy Society consensus guidelines for locally advanced carcinoma of the cervix. Part I: General principles. Brachytherapy 2012;11:33-46.
12. Viswanathan AN, Beriwal S, De Los Santos JF, Demanes DJ, Gaffney D, Hansen J, *et al.* American Brachytherapy Society consensus guidelines for locally advanced carcinoma of the cervix. Part II: High-dose-rate brachytherapy. Brachytherapy 2012;11:47-52.
13. Sturdza A, Pötter R, Fokdal LU, Haie-Meder C, Tan LT, Mazeron R, *et al.* Image guided brachytherapy in locally advanced cervical cancer: Improved pelvic control and survival in RetroEMBRACE, a multicenter cohort study. Radiother Oncol 2016;120:428-33.
14. Pötter R, Tanderup K, Kirisits C, de Leeuw A, Kirchheiner K, Nout R, *et al.* The EMBRACE II study: The outcome and prospect of two decades of evolution within the GEC-ESTRO GYN working group and the EMBRACE studies. Clin Transl Radiat Oncol 2018;9:48-60.
15. Ravikumar B, Lakshminarayana S. Determination of the tissue inhomogeneity correction in high dose rate brachytherapy for iridium-192 source. J Med Phys 2012;37:27-31.
16. Anagnostopoulos G, Baltas D, Pantelis E, Papagiannis P, Sakelliou L. The effect of patient inhomogeneities in oesophageal 192Ir HDR brachytherapy: A Monte Carlo and analytical dosimetry study. Phys Med Biol 2004;49:2675-85.
17. Bi S, Chen Z, Sun X, Dai Z. Dosimetric comparison of AcurosBV with AAPM TG43 dose calculation formalism in cervical intraductal high-dose-rate brachytherapy using three different applicators. Precis Radiat Oncol 2022;6:234-42.
18. Abe K, Kadoya N, Sato S, Hashimoto S, Nakajima Y, Miyasaka Y, *et al.* Impact of a commercially available model-based dose calculation algorithm on treatment planning of high-dose-rate brachytherapy in patients with cervical cancer. J Radiat Res 2018;59:198-206.
19. Rivard MJ, Coursey BM, DeWerd LA, Hanson WF, Huq MS, Ibbott GS, *et al.* Update of AAPM task group no. 43 report: A revised AAPM protocol for brachytherapy dose calculations. Med Phys 2004;31:633-74.
20. Briesmeister JF. MCNPTM-A General Monte Carlo n-Particle Transport Code Version 4C. Los Alamos Natl Lab; 2000.
21. Kim RY, Shen S, Duan J. Image-based three-dimensional treatment planning of intracavitary brachytherapy for cancer of the cervix: Dose-volume histograms of the bladder, rectum, sigmoid colon, and small bowel. Brachytherapy 2007;6:187-94.
22. Miglierini P, Malhaire JP, Goasduff G, Miranda O, Pradier O. Cervix cancer brachytherapy: High dose rate. Cancer Radiother 2014;18:452-7.
23. NuDat 3, National Nuclear Data Center 2004 Nuclear data from NuDat, a web-based database maintained by the National Nuclear Data Center (Brookhaven National Laboratory, Upton, NY, USA). Available from: https://www.nndc.bnl.gov/nudat3/. [Last accessed on 2023 Oct 17].
24. Sadeghi MH, Sina S, Mehdizadeh A, Faghihi R, Moharramzadeh V, Meigooni AS. The effect of tandem-ovoid titanium applicator on points A, B, bladder, and rectum doses in gynecological brachytherapy using (192) Ir. J Contemp Brachytherapy 2018;10:91-5.
25. Granero D, Vijande J, Ballester F, Rivard MJ. Dosimetry revisited for the HDR 192Ir brachytherapy source model mHDR-v2. Med Phys 2011;38:487-94.
26. Ballester F, Granero D, Pérez-Calatayud J, Casal E, Agramunt S, Cases R. Monte Carlo dosimetric study of the BEBIG Co-60 HDR source. Phys Med Biol 2005;50:N309-16.
27. López JF, Donaire JT, Alcalde RG. Monte Carlo dosimetry of the most commonly used 192 Ir high dose rate brachytherapy sources. Rev Fis Med 2011;12:159-68.
28. Granero D, Pérez-Calatayud J, Ballester F. Technical note: Dosimetric study of a new co-60 source used in brachytherapy. Med Phys 2007;34:3485-8.
29. Brachytherapy Varian. Available from: https://www.varian.com/products/brachytherapy. [Last accessed on 2023 Jun 29].

30. Arjunan M, Sekaran SC, Sarkar B, Manikandan S. A homogeneous water-equivalent anthropomorphic phantom for dosimetric verification of radiotherapy plans. J Med Phys 2018;43:100-5.
31. Gondré M, Marsolat F, Bourhis J, Bochud F, Moeckli R. Validation of Monte Carlo dose calculation algorithm for cyberknife multileaf collimator. J Appl Clin Med Phys 2022;23:e13481.
32. Eckerman KF, Cristy M, Ryman JC. The ORNL Mathematical Phantom Series. TN Oak Ridge Natl Lab; 1996.
33. Program History ORNL. Available from: https://www.ornl.gov/crpk/program-history. [Last accessed on 2023 Jul 05].
34. Normal radiological reference values Radiology Reference Article Radiopaedia.org. Available from: https://www.radiopaedia.org/articles/normal-radiological-reference-values?lang=us. [Last accessed on 2023 Jul 05].
35. Kim TG, Huh SJ, Park W. Endoscopic findings of rectal mucosal damage after pelvic radiotherapy for cervical carcinoma: Correlation of rectal mucosal damage with radiation dose and clinical symptoms. Radiat Oncol J 2013;31:81-7.
36. Hakenberg OW, Linne C, Manseck A, Wirth MP. Bladder wall thickness in normal adults and men with mild lower urinary tract symptoms and benign prostatic enlargement. Neurourol Urodyn 2000;19:585-93.
37. Soni N, Gautam B, Shvydka D, Parsai E. SU-E-T-307: Quantitative assessment of the source attenuation for the new CT-compatible titanium fletcher-suit-delclos (FSD) gynecologic applicator. Med Phys 2012;39:3774.
38. Cobalt-60 in HDR Brachytherapy – BEBIG Medical GmbH. Available from: https://www.bebigmedical.com/product/34.html. [Last accessed on 2023 Jun 25].
39. Student. The probable error of a mean. Biometrika 1908;6:1-25.
40. Sadeghi MH, Sina S, Meigooni AS. A comparison of treatment duration for cobalt-60 and iridium-192 sources with different activities in HDR brachytherapy using tandem-ovoid applicator. Iran J Med Phys 2021;18:346-51.
41. Palmer A, Hayman O, Muscat S. Treatment planning study of the 3D dosimetric differences between co-60 and ir-192 sources in high dose rate (HDR) brachytherapy for cervix cancer. J Contemp Brachytherapy 2012;4:52-9.
42. Yong JS, Ung NM, Jamalludin Z, Malik RA, Wong JHD, Liew YM, *et al.* Dosimetric impact of applicator displacement during high dose rate (HDR) cobalt-60 brachytherapy for cervical cancer: A planning study. Radiat Phys Chem 2016;119:264-71.